APPLICATION OF GENETIC ALGORITHM IN OPTIMIZING LQR CONTROL FOR BALL AND BEAM

Nguyen-Dang-Khoa Tran[1]*, Minh-Quan Nguyen[2], Tuan-Kiet Le[2], Duy-Khanh Bui[2], Thanh-Vinh Le[2], Thi-Ngoc-Thi Vo[2], Thi-Toi Nguyen[2], Ngo-Quoc-Bao Pham[2]

[1] Ton Duc Thang University (TDTU)
19Đ, Nguyen Huu Tho, district 7, Ho Chi Minh city, Vietnam
[2] Ho Chi Minh city University of Technology and Education (HCMUTE)
01- Vo Van Ngan, Thu Duc city, Ho Chi Minh city, Vietnam
* Corresponding author. E-mail: dangkhoa.tran195@gmail.com

Abstract: In this paper, we apply genetic algorithm (GA) to optimize LQR controller – a linear control algorithm which stability is guaranteed by mathematics. This searching algorithm proves its ability in finding better control parameters through generations. Our model is ball and beam (B&B) – a classical single input – multi output (SIMO) system. This system is balanced around equilibrium point in simulation.
Keywords: ball and beam, genetic algorithm, LQR control.

1. Introduction

B&B is a SIMO object that is suitable for algorithm development since it has a traditional nonlinear structure and an easy-to-produce mechanical structure. There are two different types of B&B: those with central axes, in which the motor is located in the center of the beam, and those with side axes, in which the motor is transferred to one side of the beam by a plate. The system directs the beam to move until the ball is in the desired position while maintaining equilibrium at that location. On an actual model that I constructed myself, experimental research is examined. Therefore, a reference to this model is required for subsequent studies to expand our understanding of control for this type of SIMO system.

Some authors [1] control B&B using reinforcement learning in both simulation and experiment. However, that research lacked knowledge about the dynamic equations of a genuine model. Fuzzy controllers [3], neural controllers [5]-[10], and SMC technique [6] are examples of intelligent controllers that have undergone thorough testing. However, complexity controllers have a harder time being applied to real models since they require more time and memory. In [2], GA is utilized to improve PID controllers for B&B. As a result, a good set of control parameters can control a system, but theoretically, system stability is not assured. In simulation, LQR for B&B is optimized via GA [4]. Along with PID, pole-placement, and the success of all methods in simulation, LQR control is described in [9]. However, an attempt using home-made hardware is unsuccessful. In both simulation and experiment, the LQR controller has been shown to be effective [8]. In that study, Q and R are chosen via a trial-and-error technique. Additionally, LQR optimization method is not demonstrated in that study. There are suggested LQR calibration guidelines for B&B in [7]. The quality control of the system will be impacted by modifications to each element in the matrices Q and R. However, selecting an effective set of control parameters takes time.

2. Theoretical Basis

2.1. Mathematical Model with Torque as Input

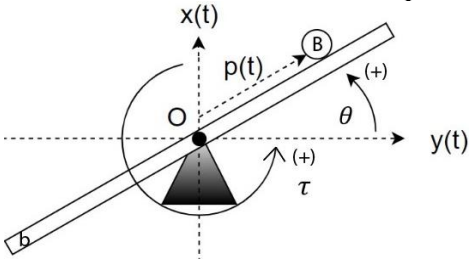

Fig. 1. B&B system's mathematical model

Tab. 1 Parameters of model system

Parameter	Description	Values
m	The ball's weight	0.09 kg
M	The beam's mass	0.45kg
L	Dimensions of beam	0.37 m
R	The ball's circumference	0.2 m
p	Position of the ball on beam, relative to the beam axis	m
θ	Beam angle with relation to the horizontal	rad
τ	Torque generated by motor, applying on the beam	Nm
u	motor voltage supply, the control signal	V
$\dot{\theta}$	velocity of the beam	rad/s
$\dot{p}$	velocity of the ball	m/s

Ball's potential energy is:

$$p_b = mgp\sin\theta \quad (1)$$

Potential energy of the beam is:

$$p_B = 0 \quad (2)$$

From (1) and (2), total system potential energy is:

$$P = p_b + p_B = mgp\sin\theta \quad (3)$$

Beam's kinetic energy is:

$$T_B = \frac{1}{2} J_B \dot{\theta}^2 \quad (4)$$

Ball's kinetic energy as it rotates around itself is:

$$T_{b\_roll\_1} = \frac{1}{2} J_b \dot{\theta}_b^2 \quad (5)$$

Rotational kinetic energy of the ball when it rotates around the beam axis is:

$$T_{b\_roll\_2} = \frac{1}{2} J_{b\_roll\_2} \dot{p}^2 \quad (6)$$

The ball's translational kinetic energy is:

$$T_{b\_translational} = \frac{1}{2} m\dot{p}^2 \quad (7)$$

From (5) - (7), total kinetic energy of ball is:

$$T_b = T_{b\_translational} + T_{b\_roll} \quad (8)$$

From (4), (8), total kinetic energy of system is:

$$T = T_b + T_B \quad (9)$$

From (3) and (9), Lagrange operator is:

$$L = T - P = \frac{1}{2} m\dot{p}^2 + mgp\sin\theta \quad (10)$$

Euler-Lagrange technique states are:

$$\frac{d}{dt}\left(\frac{\partial L}{\partial \dot{p}}\right) - \frac{\partial L}{\partial p} = 0 \quad (11)$$

where $\begin{cases} \frac{d}{dt}\left(\frac{\partial L}{\partial \dot{p}}\right) = (m + \frac{J_b}{R^2})\ddot{p} \\ \frac{\partial L}{\partial p} = mp\dot{\theta}^2 - mg\sin\theta \end{cases}$;

$$\frac{d}{dt}\left(\frac{\partial L}{\partial \dot{\theta}}\right) - \frac{\partial L}{\partial \theta} = \tau ; \begin{cases} \frac{d}{dt}\left(\frac{\partial L}{\partial \dot{\theta}}\right) = (mp^2 + J_B)\ddot{\theta} \\ \frac{\partial L}{\partial \dot{\theta}} = 2p\dot{p}\dot{\theta} - mgp\cos\theta \end{cases}$$

Thence, dynamic equations of B&B are:

$$(m + \frac{J_b}{R^2})\ddot{p} - mp\dot{\theta}^2 + mg\sin\theta = 0 \quad (12)$$

$$\Leftrightarrow \frac{mp\dot{\theta}^2 - mg\sin\theta}{m + J_b/R^2} = \ddot{p} \quad (13)$$

Thence, we obtain:

$$(mp^2 + J_B)\ddot{\theta} - 2p\dot{p}\dot{\theta} + mgp\cos\theta = \tau \quad (14)$$

$$\Leftrightarrow \frac{\tau - 2p\dot{p}\dot{\theta} + mgp\cos\theta}{mp^2 + J_B} = \ddot{\theta} \quad (15)$$

From (13) and (15), mathematical equations of system with torque as input is described below:

$$\begin{cases} \ddot{\theta} = \frac{\tau - 2p\dot{p}\dot{\theta} + mgp\cos\theta}{mp^2 + J_B} \\ \ddot{p} = \frac{mp\dot{\theta}^2 - mg\sin\theta}{m + \frac{J_b}{R^2}} \end{cases} \quad (16)$$

2.2. Mathematical Model with Voltage as Input

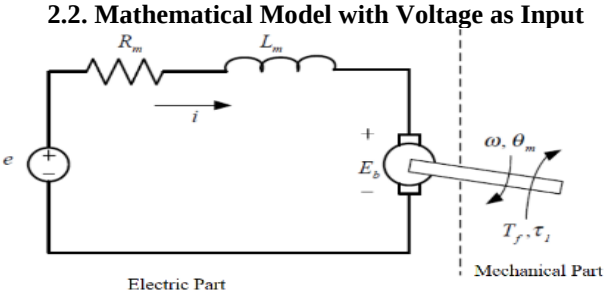

Fig. 2. DC motor's mathematical description

Tab. 2. DC motor parameters

Parameter	Description	Value
R_m	Motor resistance	Ω
K_t	Constant torque	Nm/A
K_b	Constant of the back electromotive force	V/(rad/sec)
L_m	Inductance coefficient	H
J_m	Rotor moment of inertia	kgm2
C_m	Coefficient of viscosity	Nm/(rad/sec))
τ_1	Resistance torque	Nm
T_f	Friction moment	Nm
ω	Speed of motor	rad/s
τ_m	Internal torque	Nm
θ_m	Rotation angle of motor shaft	rad

Electrical dynamic equation:

$$e = L_m\frac{di}{dt} + R_m i + E_b = L_m\frac{di}{dt} + R_m i + K_b\omega \quad (17)$$

Mechanical dynamic equation:

$$J_m\frac{d\omega}{dt} = \tau_m - T_f + C_m\omega - \tau_1 = K_1 i - T_f + C_m\omega - \tau_1 \quad (18)$$

Resistance torque:

$$\tau_1 = -J_m\frac{d\omega}{dt} + \tau_m + C_m\omega = -J_m\ddot{\theta} + K_t\frac{e - K_b\omega}{R_m} + C_m\dot{\theta} \quad (19)$$

In this paper, τ is chosen as τ_1, then, (19) is rewritten as follows:

$$\tau = -k_3\ddot{\theta} - k_2\dot{\theta} + k_1 e \tag{20}$$

where $k_1 = \frac{k_t}{R_m},\ k_2 = \frac{k_b k_t}{R_m} + C_m,\ k_3 = J_m$

Substituting (20) into (16), we obtain

$$\ddot{\theta} = \frac{-k_2\dot{\theta} - k_1 e + 2mp\dot{p} + gmpcos\theta}{(mp^2 + J_B)(\frac{k_3}{mp^2 + J_B} + 1)} \tag{21}$$

The mathematical equations of system are described below:

$$\begin{cases} \ddot{\theta} = \dfrac{-k_2\dot{\theta} - k_1 e + 2mp\dot{p} + mgpcos\theta}{(mp^2 + J_B)(\frac{k_3}{mp^2 + J_B} + 1)} \\ \ddot{p} = \dfrac{mp\dot{\theta}^2 - mg\sin\theta}{m + \frac{J_b}{R^2}} \end{cases} \tag{22}$$

where $k_1 = \frac{k_t}{R_m};\quad k_2 = \frac{k_b k_t}{R_m} + C_m;\quad k_3 = J_m;$

$J_B = \frac{1}{12}L^2 m_B;\ J_b = \frac{2}{5}R^2 m;\ \omega = \dot{\theta}$.

From (26) the mathematical equation of system

$$\dot{x} = f(x) + g(x)u \tag{23}$$

where

$$x = \begin{bmatrix} x_1 \\ x_2 \\ x_3 \\ x_4 \end{bmatrix} = \begin{bmatrix} p \\ \dot{p} \\ \theta \\ \dot{\theta} \end{bmatrix};\quad f(x) = \begin{bmatrix} f_1 \\ f_2 \\ f_3 \\ f_4 \end{bmatrix} = \begin{bmatrix} x_2 \\ \dfrac{mx_1x_4^2 - mg\sin(x_3)}{\frac{J}{R^2} + m} \\ x_4 \\ -\dfrac{k_2x_4 + 2mx_1x_2 + gmx_1cos(x_3)}{(mx_1^2 + J_B)(\frac{k_3}{mx_1^2 + J_B} + 1)} \end{bmatrix};$$

$$g(x) = \begin{bmatrix} g_1 \\ g_2 \\ g_3 \\ g_4 \end{bmatrix} = \begin{bmatrix} 0 \\ 0 \\ 0 \\ \dfrac{k_1}{(mx_1^2 + J_B)(\frac{k_3}{mx_1^2 + J_B} + 1)} \end{bmatrix}$$

3. Genetic Algorithm

With dynamic equations in (23), LQR control signal for B&B is

$$u = -Kx \tag{24}$$

This signal can be lanced system around equilibrium point

$x=x_0=[0]$; $u=u_0=0$ (25)

Matrix K is control matrix which is calculated from Matlab as:

K=lqr(A,B,Q,R) (26)

Matrices A, B are calculated by:

$$A = \left[\begin{matrix} \frac{\partial f_1}{\partial x_1} & \frac{\partial f_1}{\partial x_2} & \frac{\partial f_1}{\partial x_3} & \frac{\partial f_1}{\partial x_4} \\ \frac{\partial f_2}{\partial x_1} & \frac{\partial f_2}{\partial x_2} & \frac{\partial f_2}{\partial x_3} & \frac{\partial f_2}{\partial x_4} \\ \frac{\partial f_3}{\partial x_1} & \frac{\partial f_3}{\partial x_2} & \frac{\partial f_3}{\partial x_3} & \frac{\partial f_3}{\partial x_4} \\ \frac{\partial f_4}{\partial x_1} & \frac{\partial f_4}{\partial x_2} & \frac{\partial f_4}{\partial x_3} & \frac{\partial f_4}{\partial x_4} \end{matrix}\right]_{\substack{x=x_0 \\ u=u_0}};\quad B = \begin{bmatrix} g_1 & g_2 & g_3 & g_4 \end{bmatrix}^T \tag{27}$$

Matrices Q, R can be chosen through GA. GA which is used to optimize the LQR is described in this section. The four components K_1, K_2, K_3, K_4 of the matrix K that are have been chosen as the controller's inputs and outputs.

The following is the choice of the objective function

$$J = \sum_1^n (e^2{}_1 + e^2{}_2) \tag{28}$$

where: e_1 is the error between $p_d(t)$ desired and $p(t)$ current; e_2 is the discrepancy between $\theta_d(t)$ intended and $\theta(t)$ current; n is the number of samples used in each simulation..

The most appropriate population size was initially identified by running a number of simulations. A measurement cycle of 500 generations was looked at, with populations ranging from 2 to 50 individuals.

Tab. 3. Population size identification using GA-Related Parameters

GA component	Value
Maximum generation	500
Mutation rate	0.1
Crossover rate	0.9

$p, \dot{p}, \theta, \dot{\theta}$ The average aim of each run reduces until it achieves its local maximum because the GA selection process includes more potential candidates with favorable genes as population size rises.

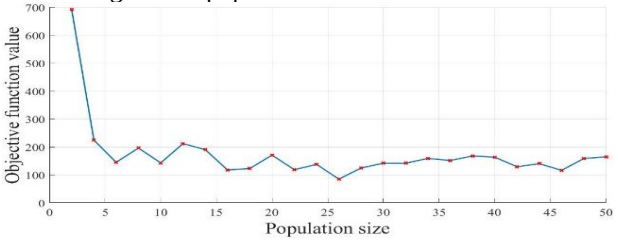

Fig. 3. Population size and average object function value in 500 generation

A large number of runs with crossover probabilities between 0.1 and 0.9. It is evident that as the crossover rate increases from 0.1 to 0.2, the average objective function value of each run lowers significantly. It can be explained by the possibility that crossover processes will preserve the better genes from the ancestors of the parents in order to enhance the performance of following generations. The crossover probability position was 0.9 when the average target reached its peak.

Tab. 4. Crossover rate detection using GA-Related Parameters

GA component	Value
Maximum generation	500
Mutation rate	0.1
Population size	26

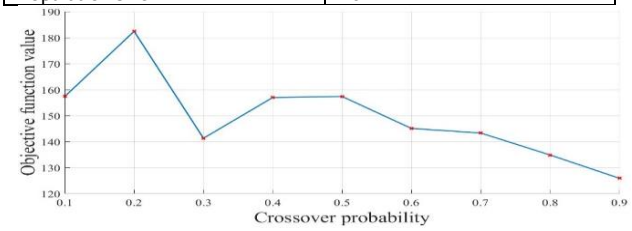

Fig. 4. Probability of crossover in 500 generations when population is 26

The population size selected was 26, and the crossover probability position was adjusted to 0.9, as shown in Fig. 4. Fig. 5 illustrates the process of choosing the appropriate mutation probability by plotting the best average objective function value of each run at various mutation probabilities.

Tab. 5. GA-Related variables determining the rate of mutation

GA component	Value
Maximum generation	500
Mutation rate	0.9
Population size	26

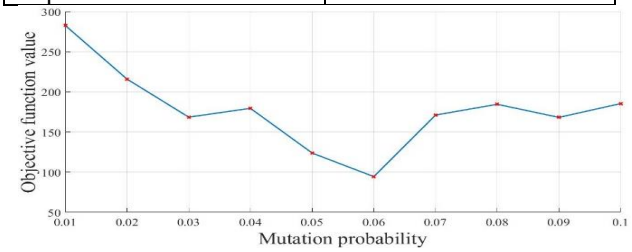

Fig. 5. Probability of mutation in 500 generations with a population size of 26

Tab. 6. GA-Related parameters of system

GA component	Value
Population size	26
Chromosome count for each individual	4
Max generation	500
Mutation rate	0.06
Crossover rate	0.9

GA programs calculate the outcome after roughly 500 generations. The value of the objective function is then displayed in Fig. 6 after that.

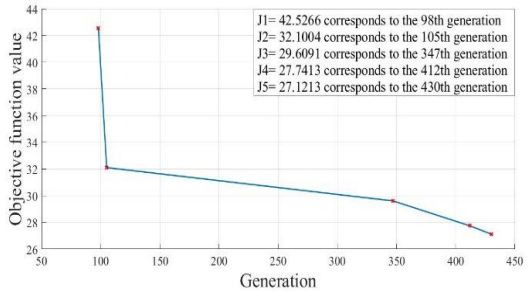

Fig. 6. Objective function value in 500 generations

4. Results

This chapter shows the simulation and experiment results. Initial values of system are as follows:

$$x = \left[x_1\ x_2\ x_3\ x_4\right]^T = \left[p\ \dot{p}\ \theta\ \dot{\theta}\right]^T = \left[-0.15\ 0\ 0\ 0\right]^T \quad (29)$$

The beam is horizontally balanced, and the ball is far from the static operating point.

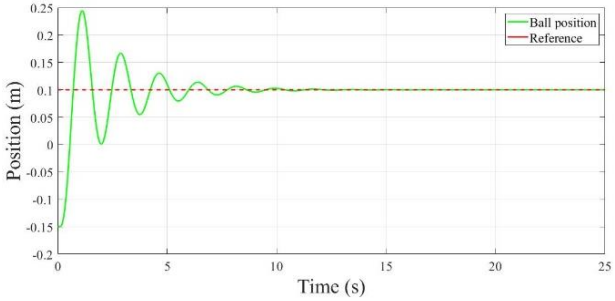

Fig. 7. Ball position simulation at the 98th generation results

Tab. 7. Post-tuning performance parameters of ball position at the 98th generation

POT (%)	Settling time (s)	Steady state error (m)	Rise time (s)	Peak time (s)
144.6	11.27	0	0.3189	1.12

The ball's position's settling time in Fig. 7 is 11.27 seconds. The ball's position oscillates between 0.245 m and -0.15 m in height.

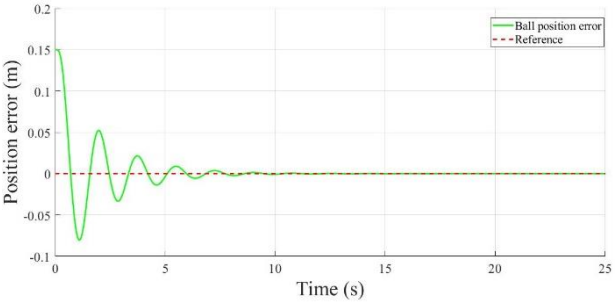

Fig. 8. Ball position error simulation at the 98th generation results

After 11.27 seconds, the ball's position inaccuracy in Fig. 8 is equal to zero.

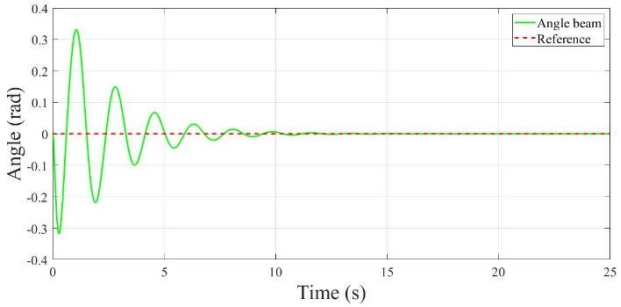

Fig. 9 The 98th generation's beam angle as predicted via simulation

Tab. 8. Post-tuning performance parameters of beam angle at 98th generation

POT (%)	Settling time (s)	Steady state error (m)	Rise time (s)	Peak time (s)
Ø	12.94	0	Ø	1.06

The beam angle's settling time in Fig. 9 is 11.8 seconds. The angle of the beam oscillates between -0.3224 rad and 0.1703 rad in amplitude.

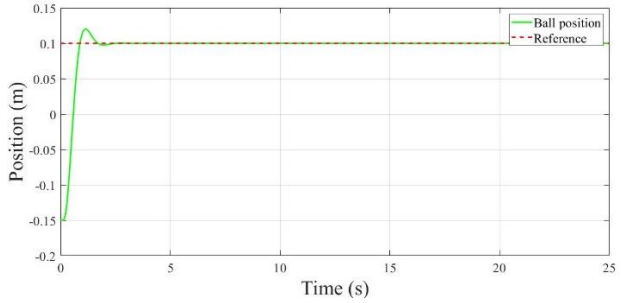

Fig. 10. Ball position simulation at the 105th generation results

Tab. 9. Post-tuning performance parameters of ball position at 105th generation

POT (%)	Settling time (s)	Steady state error (m)	Rise time (s)	Peak time (s)
20	6.88	0	0.483	1.12

The ball's position in Fig. 10 settled after 6.88 s. The ball's position oscillates between 0.12 m and -0.15 m in height.

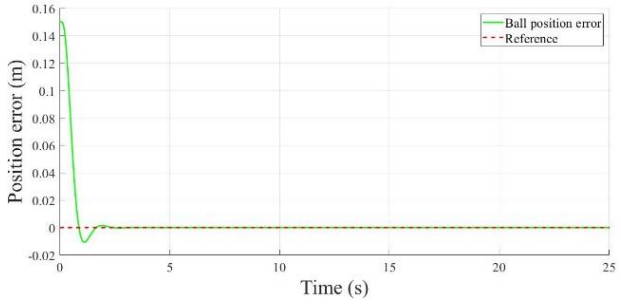

Fig. 11. Ball position error simulation at the 105th generation results

After 6.88 seconds, the ball's position inaccuracy in Fig. 11 is equal to zero.

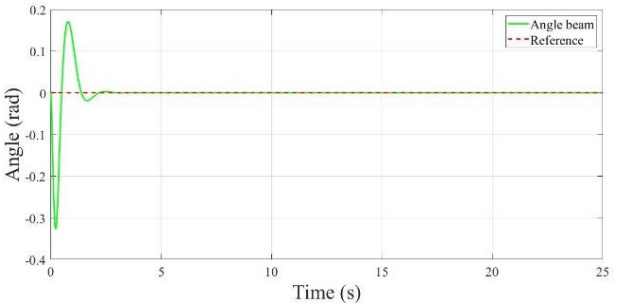

Fig. 12. The 105th generation's beam angle as predicted via simulation

Tab. 10. Post-tuning performance parameters of beam's angle at 105th generation

POT (%)	Settling time (s)	Steady state error (m)	Rise time (s)	Peak time (s)
Ø	11.8	0	Ø	7.8

The beam angle's settling time in Fig. 12 is 6.36 s. The angle of the beam oscillates between -0.188 rad and 0.0476 rad in amplitude.

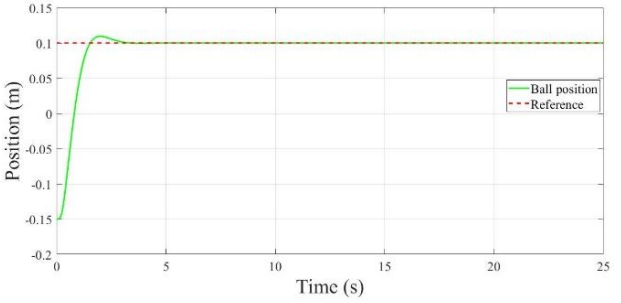

Fig. 13. 347th generation simulation result for ball position

Tab. 11. Post-tuning performance parameters of beam angle at 347th generation

POT (%)	Settling time (s)	Steady state error (m)	Rise time (s)	Peak time (s)
9.4	6.01	0	0.89	1.95

The ball's position in Fig. 13 settled in 6.01 s. The position of the ball oscillates between 0.1094 m and -0.15 m in amplitude.

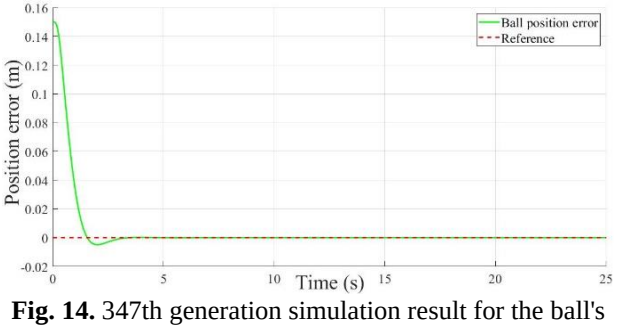

Fig. 14. 347th generation simulation result for the ball's location error

After 6.01 seconds, the ball's position inaccuracy in Fig. 14 is equal to zero.

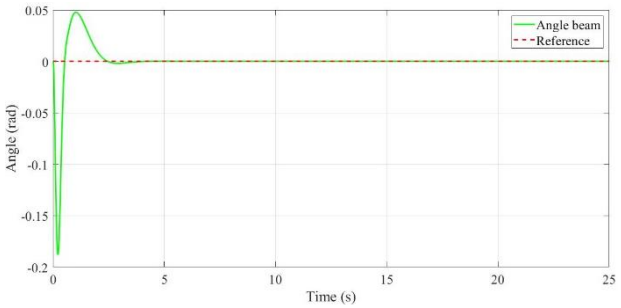

Fig. 15. Simulation result for beam's angle at the 347th generation

Tab. 12. Post-tuning performance parameters of beam angle at 347th generation

POT (%)	Settling time (s)	Steady state error (m)	Rise time (s)	Peak time (s)
Ø	6.36	0	Ø	1.01

In Fig. 15, the beam angle's settling time is 12.53 s. The beam's angle oscillates with an amplitude ranging from -0.018 rad to 0.004 rad..

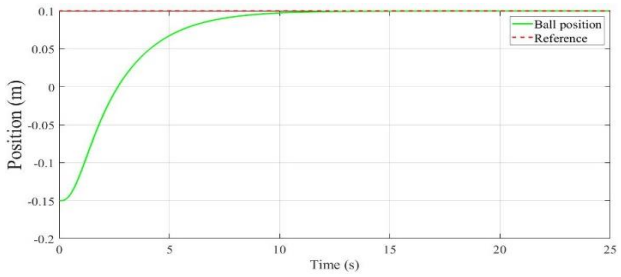

Fig. 16. Simulation result for ball's position at the 412th generation

Tab. 13. Post-tuning performance parameters of beam angle at 412th generation

POT (%)	Settling time (s)	Steady state error (m)	Rise time (s)	Peak time (s)
0	12.88	0	5.61	Ø

The ball's position in Fig. 16 settled in 12.88 s. The ball's position oscillates between 0.1 m and -0.15 m.

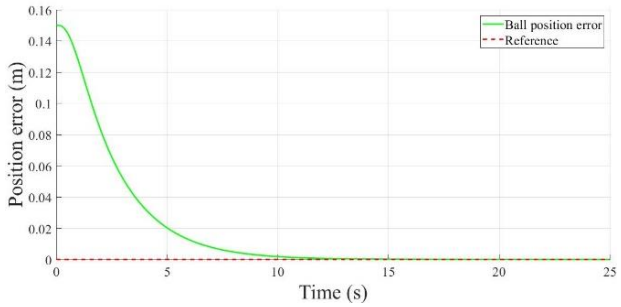

Fig. 17. The 412th generation's simulation result for ball's location error

After 12.88 seconds, the ball's position inaccuracy in Fig. 17 is equal to zero.

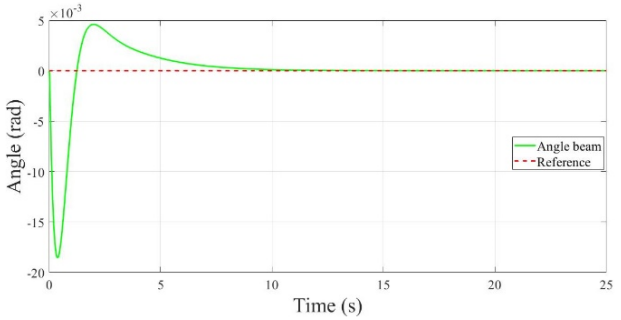

Fig. 18. Simulation result for beam's angle at 412th generation

Tab. 14. Post-tuning performance parameters of beam's angle at 412th generation

POT (%)	Settling time (s)	Steady state error (m)	Rise time (s)	Peak time (s)
Ø	12.53	0	Ø	1.95

The beam angle's settling time in Fig. 18 is 12.53 s. The angle of the beam oscillates between -0.018 rad and 0.004 rad in amplitude.

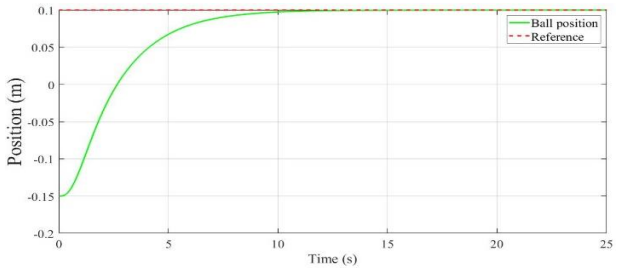

Fig. 19. Ball position simulation at the 430th generation results

Tab. 15. Post-tuning performance parameters of beam angle at 430th generation

POT (%)	Settling time (s)	Steady state error	Rise time (s)	Peak time (s)
0	12.8	0	56.2	Ø

Ball's position in Fig. 19 settled after 12.8 s. The ball's position oscillates between 0.1 and -0.15 meters.

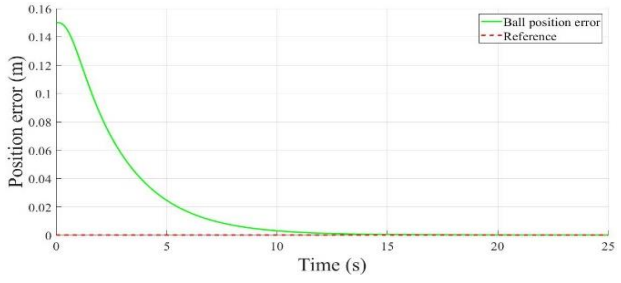

Fig. 20. Ball position error simulation at 430th generation results

After 12.8 seconds in Fig. 20, the ball's location error reaches zero.

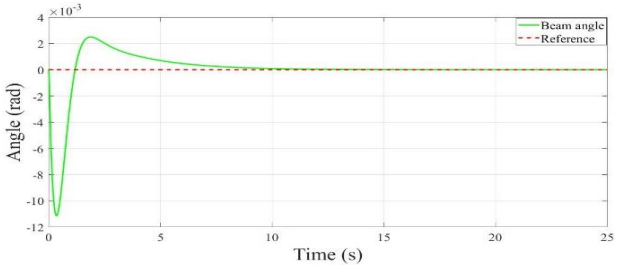

Fig. 21. Simulation result for beam's angle at 430th generation

Tab. 16. Post-tuning performance parameters of beam's angle at 430th generation

POT (%)	Settling time (s)	Steady state error	Rise time (s)	Peak time (s)
Ø	12.44	0	Ø	1.89

Beam angle's settling time in Fig. 21 is 12.44 s. Angle oscillations range from -0.011 rad to 0.002 rad in amplitude.

5. Conclusions

Through the study, the preparations is demonstrated such as: building the system of dynamic equations of the BTTG system with the input voltage, proving the controllability of the system, creating the basis for building the system's stable condition at a static working point, presenting the mathematical structure of an LQR conditional and how to quickly calculate control parameters through Matlab tool, building experimental model of B&B, applying GA to optimize LQR on simulation to confirm the successful optimization of GA for LQR algorithm, demonstrating the optimization of GA in the optimization of LQR conditionals experimentally, bring the analysis and survey of optimization using GA to LQR in this case.

Acknowledgement

We want to give thanks to PhD. Van-Dong-Hai Nguyen (HCMUTE) due to his support in giving ideas for us to complete this contribution.

6. References

[1] Shixuan, Y. et al.: "Research on Solving Nonlinear Problem of Ball and Beam System by Introducing Detail-Reward Function", Symmetry, 2022.
[2] Ali A.T. et al: "Design and Implementation of Ball and Beam System Using PID Controller", Automatic Control and Information Sciences, pp. 1-4, 2017.
[3] Gergely B. et al: "Establishing metrics and control laws for the learning process: ball and beam balancing", Biological Cybernetics, pp. 114, 2020.
[4] Le A.T. Tran N.D.K: "Applying a Genetic Algorithm to optimize Linear Quadratic Regulator for Ball and Beam system", The 7th International Conference on Advanced Engineering – Theory and Applications, Ton Duc Thang University, 2022.
[5] Liqing G., Yongxin L: "Design of BP neural network controller for ball-beam system", IEEE Advanced Information Management, Communicates, Electronic and Automation Control Conference (IMCEC), 2016.
[6] Muhammad I. et al.: "Sliding mode control design for stabilization of underactuated mechanical systems", Advances in Mechanical Engineering, 2019.
[7] Nguyen X.C. et al.: "Building Quasi-Time-Optimal Control Laws For Ball And Beam System", 3rd International Conference on Recent Advances in Signal Processing, Telecommunications & Computing (SigTelCom), 2019.
[8] Nguyen X.C. et al.: "The design of a quasi-time optimal cascade controller for ball and beam system", IOP Conference Series: Materials Science and Engineering, pp. 1029, 2021.
[9] Valluru S.K. et al.: "Prototype design and analysis of controllers for one dimensional ball and beam system", IEEE 1st International Conference on Power Electronics, Intelligent Control and Energy Systems (ICPEICES), 2016.
[10] Wang Q. et al.: "Evolving a neural controller for a ball-and-beam system", Proceedings of 2004 International Conference on Machine Learning and Cybernetics (IEEE Cat. No.04EX826), 2004.